INTERNATIONAL JOURNAL OF HYDROGEN ENERGY 39 (2014) 2236–2245

Available online at www.sciencedirect.com

ScienceDirect

journal homepage: www.elsevier.com/locate/he

Fuel cell diagnosis method based on multifractal analysis of stack voltage signal

D. Benouioua [a,b,*], D. Candusso [a,b], F. Harel [b,c], L. Oukhellou [d]

[a] IFSTTAR/COSYS/LTN, 25 Allée des marronniers, F-78000 Versailles Satory, France
[b] FR FCLAB, UTBM Bât. F, Rue Thierry Mieg, F-90010 Belfort Cedex, France
[c] Université de Lyon, IFSTTAR/AME/LTE, 25 Avenue François Mitterrand, Case 24, Cité des mobilités, F-69675 Bron Cedex, France
[d] Université Paris Est, IFSTTAR/COSYS/GRETTIA, 14-20 Boulevard Newton, Cité Descartes, Champs sur Marne, F-77447 Marne la Vallée Cedex 2, France

ARTICLE INFO

Article history:
Received 12 September 2013
Received in revised form
30 October 2013
Accepted 17 November 2013
Available online 22 December 2013

Keywords:
PEM fuel cell
Failure
Singularity spectrum
Diagnosis

ABSTRACT

Measuring local singularities on voltage signal transmits valuable information about the evolving dynamics of non-stationary and nonlinear processes in fuel cell systems. This paper deals with wavelet transform combined with multifractal formalism proposed for PEMFC behavior analysis. The proposed method combines the capability of wavelet transform to produce high coefficients on the singular points of signals and the ability of multifractal formalism to measure the singularity strength via the wavelet coefficients. This method is applied in order to discriminate the voltage signals acquired on a PEMFC operated in different conditions. The average multifractal spectrum estimated on voltage signals acquired at nominal operating conditions is compared to those measured for poor operating conditions considered as fault modes.

The purpose of this study is threefold. First, the multifractal structure of the fuel cell voltage signal is highlighted. Second, the singularities signature of severe operating conditions is revealed through the multifractal spectrum. Third, the wavelet based multifractal spectrum can be considered as a pertinent tool for the non-intrusive diagnosis of fuel cells.

1. Introduction and motivation

Several types of Fuel Cells (FCs) are being investigated by research laboratories and different technologies are currently under intensive development with the aim to ensure a possible large-scale commercial viability. Numerous research works done in this field focus on the optimization of the operation, the performance and adaptation of FCs in transportation, stationary and portable applications [1–4]. In particular, Proton Exchange Membrane Fuel Cell (PEMFC) has received much attention in the last two decades and its development reached a more mature phase for ground vehicle applications [5,6]. PEMFC has the advantage of yielding high

* *Corresponding author*. IFSTTAR/COSYS/LTN, 25 Allée des marronniers, F-78000 Versailles Satory, France. Tel.: +33 (0) 3 84 58 36 13; fax: +33 (0) 3 84 58 36 36.
E-mail addresses: djedjiga.benouioua@ifsttar.fr (D. Benouioua), denis.candusso@ifsttar.fr (D. Candusso), fabien.harel@ifsttar.fr (F. Harel), latifa.oukhellou@ifsttar.fr (L. Oukhellou).
0360-3199/$ – see front matter
http://dx.doi.org/10.1016/j.ijhydene.2013.11.066

power densities at relatively low operating temperatures, with small installation sizes, lightweights and relatively lower costs.

As any other device, it is necessary to know when and why a FC is not operating properly. This information is needed for the control and monitoring of onboard systems to prevent failure, or to correct poor operating conditions before that any component is damaged. Various internal and external factors are known to affect the useful life of PEMFCs. When any FC operational parameters (e.g. gas pressures and stoichiometry rates) are deflected from their nominal values, the stack performance can be strongly impacted. Stack and/or cell voltage changes can reveal some damage phenomena and failure modes such as electrode flooding, membrane drying, gas leakage, loss of electroactive surface area [7–10]. In this context, the proposal of diagnostic tools aims to provide potential solutions for improving stack durability, reliability, efficiency and for optimizing system development. Electrochemical characterization techniques such as polarization curve record [11], current interruption method [12], and Electrochemical Impedance Spectroscopy (EIS) [13,14] have been widely employed for the diagnosis of FCs. These methods are efficient in the detection of various failure modes, but have limitations for real-time applications. For example, it is difficult to implement EIS methods in real FC applications since accurate controls of FC current or voltage, and thus additional and expensive equipment (e.g. electrochemical impedance spectrometer) are required. Beyond the experimental data acquisition process and the measurement instruments needed to ensure a proper diagnosis, numerous publications have proposed signal processing based methods as diagnostic FC tools: Fourier transform [15], wavelets [16], neural network [17] and Bayesian network [18].

In this context, we chose to consider only the "free" evolution of FC stack voltages (i.e. without introducing any additional load current perturbation or solicitation as it is the case for EIS measurement) and to apply an original method, namely the multifractal analysis. Many natural and artificial phenomena such as turbulence, diffusion limited aggregates, and electrical discharges [19] exhibit multifractality. Since these phenomena are highly nonlinear and non-stationary, regular analyses such as Fourier decomposition cannot always characterize them effectively. The multifractal analysis is introduced to avoid this limit. It consists in computing the singularity strengths of a signal through the Hölder exponent.

Multifractal analysis has been developed in many directions since its introduction such as pathology diagnostic in the medical field [20–22] and has been also used in some applications of health monitoring: the detection of fatigue cracks [23] and the fault diagnosis for rotating machines [24]. In Refs. [23], the authors have used singularity spectrum to identify the crack initiation site of a broken elastomer piece used in automobile application. In Refs. [24], multifractal detrended fluctuation analysis is proposed to identify faulty rolling bearings from vibration data. Some progress has been achieved concerning the domain of validity of the multifractal formalism, both in the deterministic and random frameworks [25]. Very few works that combine fractals and FC characterization have been identified in the scientific literature. Most of them are dedicated to the optimization of electrolyte and membrane shape and composition. So, Tanner and Work showed in their paper [26] that a fractal (self-similar) structure of electrode shape optimizes and facilitates electrons transport for thin electrolyte supported FCs.

This paper presents a non-intrusive diagnostic tool based on local singularities analysis of FC voltage using multifractal formalism. The abrupt changes in a temporal signal are called singularities; they represent cusps and oscillations in the data. These singularities deliver very useful information on physical system (or signal source) and a characterization of their strength is obtained with the Hölder exponent h [27]. Multifractal analysis of irregular signals based on the Wavelet Transform Modulus Maxima (WTMM) was recently introduced [28]. Indeed, the WTMM representation is emphasized as a very efficient and accurate numerical tool for scanning the singularities of mathematics or physical signals. The principle of this method is to determine the singularity spectrum (or multifractal spectrum) of the studied signal. It consists in associating to each Hölder exponent h (local regularity exponent) the Hausdorf dimension of the sets of points which exhibit the same value of h. The Hölder exponent estimation is given by the continuous WTMM of the signal; more details on this mathematical description can be found in Refs. [29,30]. This approach provides a tool which describes geometrically and statistically the distribution of singularities on the signal support. The proposed FC diagnosis tool is developed by measuring the singularities spectrum of voltage signal, which qualify and quantify the cause-effect (failure-singularity strength) relationship among the poor operating conditions and the stack voltage. The analysis focuses on the ability to identify the signature of severe operating conditions from the morphology of stack voltages. For this purpose, some experimental tests were carried out on a 8 cell PEMFC stack in different operating conditions; more details about the experimental are given in Part 2 of this paper. In Part 3, we outline the theoretical basis of multifractal analysis based on WTMM. Part 4 is devoted to the presentation and discussion of the results obtained. Finally, this paper will be completed with major conclusions.

2. Experimental and material

In the present study, an 8 cell PEMFC was operated under a variety of conditions using an in-house self-developed test bench dedicated to electrical power levels less than 1 kW.

2.1. *Synopsis of the investigated fuel cell*

The experimented FC is manufactured by CEA LITEN. It has been designed for automotive applications. It is made of metallic gas distributor plates. Its size is 220 mm × 160 mm × 186 mm and the electrode active surface is 220 cm^2. A summary of the nominal operating conditions is given in Table 1.

2.2. *Overview of the FC test system*

The FC test bench has been developed in-lab and is dedicated to the characterization of FC for power less than 1 kW (see. Fig. 1). It includes a complete gas conditioning system, the

Table 1 – Summary of the nominal operating conditions for the experimented PEMFC.

Coolant flow: water	2 l/min
Anode stoichiometry (H_2)	1.5
cathode stoichiometry (air)	2
Absolute pressure of input H_2	150 kPa
Absolute pressure of input air	150 kPa
Maximum differential of the pressure (anode–cathode)	30 kPa
Temperature of the output of the cooling circuit	80 °C
Anode relative humidity	50%
Cathode relative humidity	50%
Current	110 A
Current density	0.5 A cm^{-2}

electric/electronic management system, the electronic load, the FC primary water circuit dedicated to the control of the temperature inside the stack and the data acquisition system. Gas flows are controlled upstream by thermal mass flow controller and the pressure is piloted downstream by back pressure valves. Humidification is based on bubblers on both oxidant and reactant lines. Gas inlets can be fed either by reactant gases (air and hydrogen) or nitrogen. The test bench temperature control circuit consists of a primary circuit filled with deionized water and two secondary circuits, one for cooling, the other for heating. Primary and secondary circuits are linked between exchangers. More descriptions of the test bench are given in detail in Ref. [31].

The monitoring and controls of the FC test bench parameters are done through National Instruments materials and dedicated softwares developed with Labview™.

2.3. *Experimental protocol*

A set of tests was performed on the FC stack; these tests duplicate various failures which are representative of the application environment (electric vehicle or stationary generator), and it includes:

- Failure of the air supply system of the FC (cathode stoichiometry factor FSC≠2).
- Failure of the hydrogen supply system of the FC (anode stoichiometry factor FSA≠1.5).
- Failure of the inlet gases pressure (P≠1.5 bars).

More details on the operating conditions are summarized in Table 2.

3. Singularity spectrum calculation

Fractals are rough or fragmented geometric shape that can be subdivided in parts, each of which is a reduced copy of the whole. These fragmented patterns can be characterized using the increase of a measure $\mu(B_x(s))$ at different scales, where $B_x(s)$ is the volume element of size s and centered at x. This element is a square box in the case of box-counting method. If $s \to 0^+$, the measure $\mu(B_x(s))$ is defined as:

$$\mu(B_x(s)) \sim s^{h(x)} \quad (1)$$

where $h(x)$ is the local singularity strength of the measure μ at a given x.

The direct determination by numerical computing of the singularity h of the real signal proves to be difficult because the number of definitions to compute it is infinite. A formula, named "multifractal formalism" has been established by Parisi and Frisch [32] in order to compute the singularity spectrum. The multifractal formalism was then defined by:

$$D(h) = \inf_{q \in R}(qh - \tau(q) + c) \quad (2)$$

$D(h)$ is the fractal dimension of E_h (E_h is the set of points that exhibit the same irregularity strength h), c is a constant and $\tau(q)$ is the scaling function. The pairs $(q, \tau(q))$ and $(h, D(h))$ are linked by the Legendre transform (2).

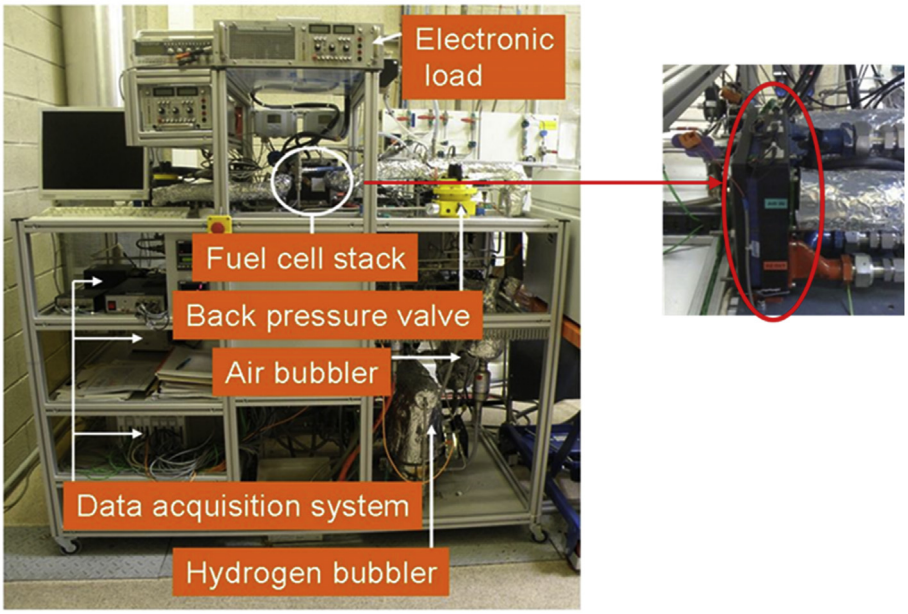

Fig. 1 – 1 kW test bench of the FC test platform in Belfort (on the left) and CEA 8 cell stack (on the right).

Table 2 – Operating parameters applied for the experimentation.

Parameters value	Nominal conditions	Cathode flow failure	Anode flow failure	Inlet gases pressure failure
FSC	2	1.3	2	2
FSA	1.5	1.5	1.3	1.5
P (bars)	1.5	1.5	1.5	1.3

The multifractal spectrum $D(h)$ of self-similar signals is a concave curve and can therefore be calculated from $\tau(q)$. This statistical tool is used to identify the deviations in fractal structure within time periods with large and small fluctuations.

Multifractal measures given by the formula (2) describe the behavior of the objects not only at different scales s, but also for different statistical moments q. The parameter q serves as a "microscope" for exploring different regions of the singular measurement [33]:

- For values $q > 0$, the strongly singular measures are enhanced.
- For values $q < 0$, the less singular areas are emphasized.

Thus, the idea of covering the support μ is also applied in different moments, which leads to the definition of the following partition function:

$$Z(q,s) = \sum_{i=1}^{N(r)} (\mu(B_i(s)))^q \tag{3}$$

where $N(r)$ is the number of elements (circle or square).

For each $q \in R$, the scaling exponent $\tau(q)$ measures the asymptotic decay of $Z(q,s)$ at fine scales s :

$$\tau(q) = \lim_{s\to 0}\left(\inf\left(\frac{\log Z(q,s)}{\log s}\right)\right) \tag{4}$$

This typically means that:

$$Z(q,s) \sim s^{\tau(q)} \tag{5}$$

One of the powerful properties of the Wavelet Transform (WT) is that the strength of the singularities points in the signal can be detected and measured at multiple scales through the local maxima coefficients (WTMM) [25]. The other fundamental advantage of using WT is that the skeleton defined by the WTMM provides an adaptive space-scale partitioning from which we can extract the $D(h)$ singular spectrum. It is well adapted to reveal the hierarchy that governs the spatial distribution of singularities of multifractal measures.

This specification of the WTMM is related to the partition function given by the formula (3), replaced by:

$$Z(q,s) = \sum_{l\in L(s)}\left(\sup_{(u,s)\in l, s\le s}\left|W_\psi(X)(u,s)\right|^q\right) \tag{6}$$

where $W_\psi(X)$ is the continuous wavelet transform of the signal X, using mother wavelet of type ψ at a location u and a scale s :

$$\forall u\in R, \forall s>0, W_\psi(X)(u,s) = \frac{1}{\sqrt{s}}\int_R X\psi\left(\frac{x-u}{s}\right)dx \tag{7}$$

The major implementation steps of the multifractal spectrum computation based on WTMM method can be formulated as follows:

i. Calculate the Wavelet Transform (WT) of the signal at multiple scales.
ii. Find the local maxima of WTs in each scale.
iii. Chain the wavelet maxima across scales.
iv. Compute the partition functions $Z(q,s)$ using the formula (6).
v. Compute $\tau(q)$ with a linear regression of $log_2 Z(q,s)$ as a function of $log_2 s$:

$$\log_2 Z(q,s) \approx \tau(q)\log_2 s + K(q)$$

vi. Compute the spectrum of singularity $D(h)$ using the formula (2).

The applied wavelet must satisfy the regularity criterion which is related to the number of vanishing moments defined by the formula (8).

$$\forall k = 0\,1\cdots N-1, \quad \int_R x^k\psi(x)dx = 0 \tag{8}$$

ψ is a wavelet with N vanishing moments. The best wavelet examples are the derivatives of the Gaussian. In our study the Mexican hat wavelet (2nd derivative of the Gaussian) is applied and $0 \le h \le N$.

To illustrate the different stages of calculating the singularity spectrum, two examples of signals are reported in Fig. 2. These examples simulated using the FRACLAB Toolbox display the differences between a monofractal and a multifractal signals through the singularity spectrum shape and width.

The first signal is a famous fractal curve generated by the Weierstrass function $W_h(x)$ (see Fig. 2(a)) (left column)) which is Hölder continuous of exponent h with $h = 0.7$ and exhibits self-similarity (i.e. every zoom is similar to the global plot). This function has the property that is continuous everywhere but differentiable nowhere and at each point the pointwise Hölder exponent is equal to h, equivalently as:

$$\mathcal{W}_h(x) = \sum_{n=0}^{\infty} a^{-nh}\cos(b^n\pi x) \tag{9}$$

where$0 \le a \le 1$, b is a positive odd integer and $ab > 1 + 3/2\pi$.

The second signal describes a multifractal structure represented by a Multifractional Brownian Motion (MBM) given at the top of Fig. 2(b)) (right column). A key feature of the MBM is that sample path fluctuation is described by a Hölder function $h(x)$ rather than just a single number:

$$\mathrm{MBM}(x) = \int_{-\infty}^{0}\left[(x-u)^{h(x)-1/2} - (-u)^{h(x)-1/2}\right]\cdot d\omega(u) + \int_0^x (x-u)^{h(x)-1/2}\cdot d\omega(u) \tag{10}$$

where ω denotes a pure *white noise* process with zero mean and the varianceσ^2.

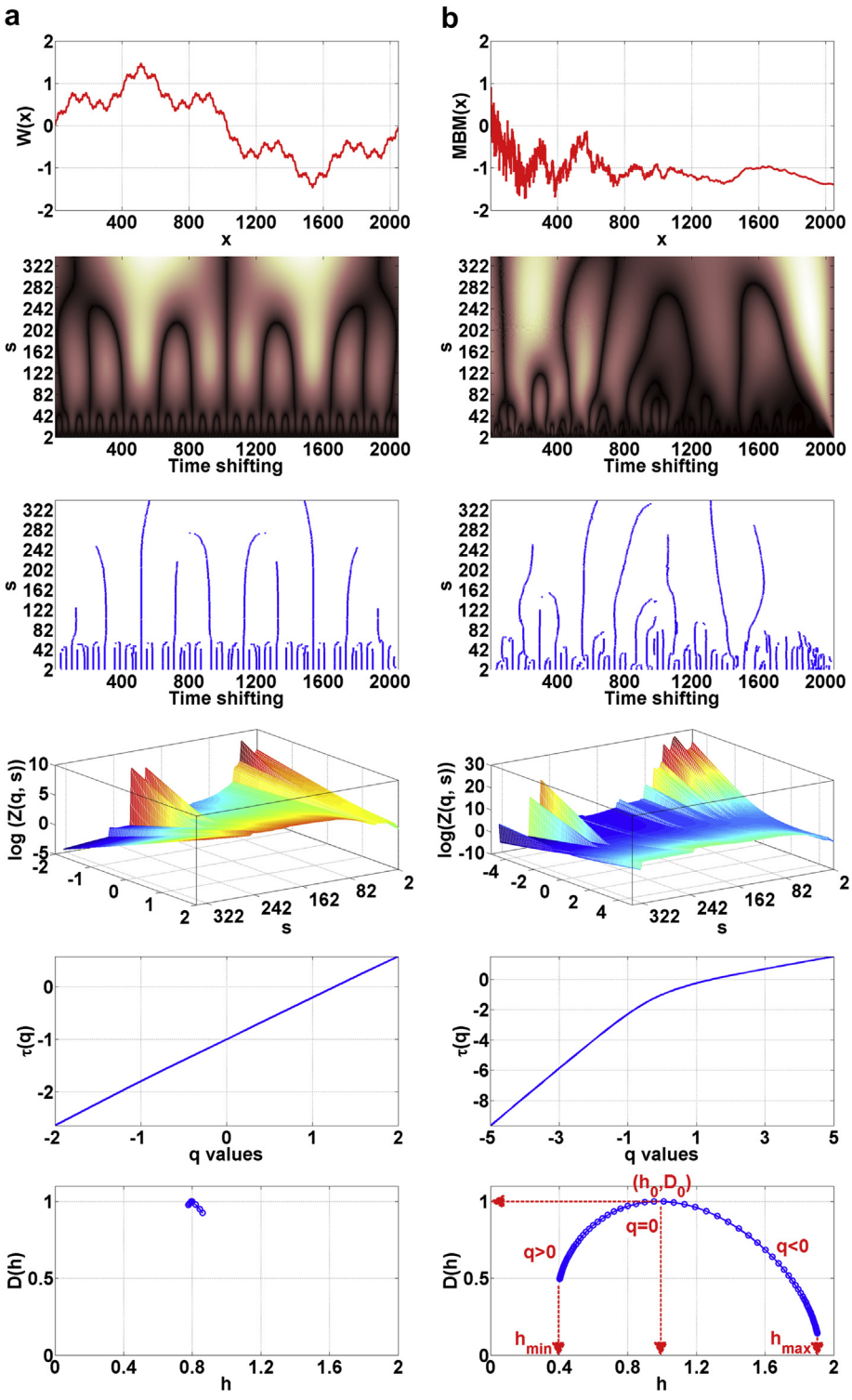

Fig. 2 – Illustration of the different steps of the multifractal spectrum computation based on WTMM of: a) Weierstrass fractal signal with $h = 0.7$ and $n = 50$ (left column) and b) multifractional Brownian Motion Signal with Hölder function $h(x) = 0.1 + 0.8x$ and $\sigma = 1$ (right column).

The increments of MBM are not stationary and the process is no more self-similar.

As shown in Fig. 2(a)) (left column), the monofractal Weierstrass signal has a scaling exponent $\tau(q)$ with a linear q-dependency that leads to a constant h_q that is the tangent slope of $\tau(q)$. The constant h_q reduces the multifractal spectrum $D(h)$ to a small arc (theoretically, its represented by a single point).

In contrast, the multifractal signal MBM(x) provides $\tau(q)$ values with a curved q-dependency. The obtained

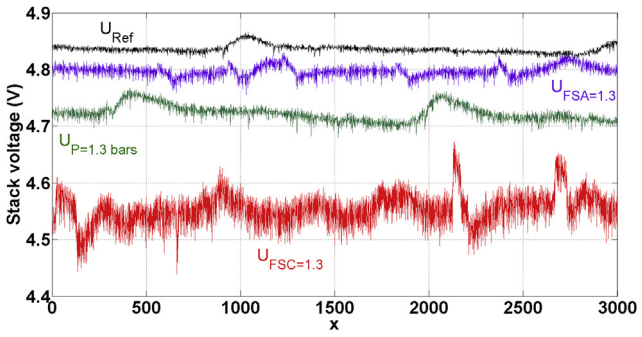

Fig. 3 – Examples of stack voltages acquired at nominal conditions (Ref) and in poor operating conditions (FSC = 1.3, FSA = 1.3, and P = 1.3 bars).

multifractal spectrum is a large concave arc (see Fig. 2(b): right column).

Therefore, the four pertinent multifractal parameters (h_0, h_{min}, h_{max} and $\Delta h = h_{max} - h_{min}$) can be used to quantitatively recognize possible differences in singularity spectra stemming from different signals. The parameter h_0 indicates the dominant singularity strength in the signal. If h_0 is low, the signal is more irregular.

Also, the strong measure of multifractality is revealed by the broad range of Hölder exponents, i.e. the width values Δh. So, the larger the spectrum width is, the more non-uniform the signal morphology and the richer the signal in self-similar structures.

4. Multifractal analysis of voltage signals

It is reasonable to assume that the test of the PEMFC under poor operating conditions affects the morphology of the stack voltage signals. In this frame, the investigation of the temporal fluctuations observed in the FC voltage signals could provide direct information on the FC dynamics and state-of-health. Therefore, to characterize these signals quantitatively, suitable and robust techniques are needed to extract possible features hidden in these complex fluctuations.

In this work, we adopt the multifractal analysis of voltage signal in order to extract and identify the singularity signature of defaults related to the imposed operating conditions.

The multifractal analysis is performed from ten sequences of stack voltage signal acquisition. The data are carried out at a frequency close to 11 Hz. Each sequence lasts almost five minutes and comprises about 3000 points. The choice of the analyzed voltage size is related to J. W. Kantelhardt work [34] where the results of the statistical standard errors of h according to the sample number of the signal are presented. The data acquisition set done in 10 sequences is repeated for four different operating conditions. The first data set (10 stack voltage signals) is measured under the nominal operating conditions listed in Table 1 and it is considered as the reference data set. The three other sets are acquired under more severe operating conditions linked with possible FC generator faults, namely:

- failure of the air supply subsystem in the FC generator (leading to the cathodic stoichiometric factor FSC = 1.3),
- failure of the hydrogen supply subsystem (leading to the anode stoichiometry factor FSA = 1.3),
- failure of pressure control subsystem (inducing inlet gas pressures P = 1.3 bars).

Additional details about these severe conditions are given in Table 2.

Some examples of stack voltage signals recorded in the four different operating conditions are plotted in Fig. 3. As we can see at first sight, each operating default gives its own stamp on the morphology of the stack voltage.

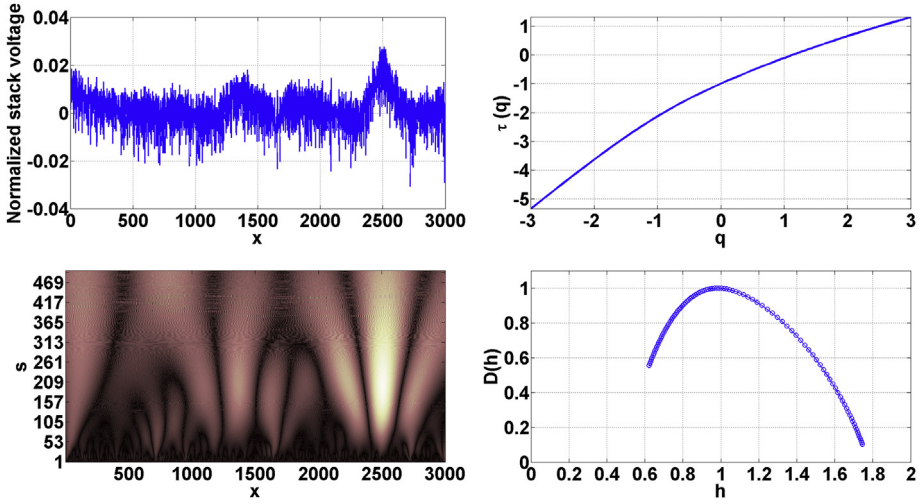

Fig. 4 – Singularity spectrum of a normalized stack voltage signal measured at nominal operating conditions (top left), with resulting curves of: map of wavelet coefficients using 2nd derivative of Gaussian (bottom left) for scales = 1:2:(L/6) with L = length (voltage signal), scaling function for $q = -3{:}3$ (101 values) (top right) and concave multifractal spectrum (bottom right).

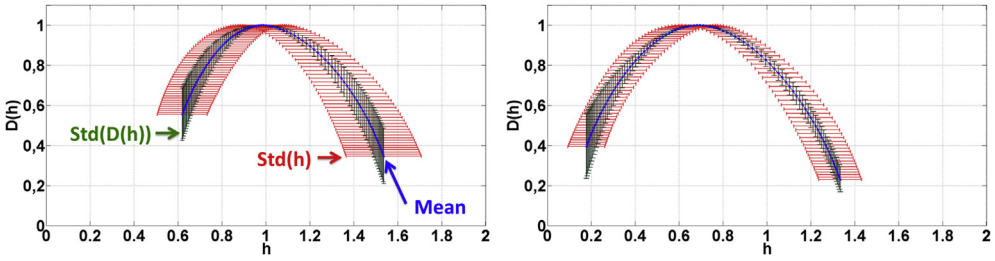

Fig. 5 – Average singularity spectra ± std values computed on 10 stack voltage signals acquired under: nominal operating conditions (left side) and poor operating conditions with FSC = 1.3 (right side).

The singularity spectrum computed using the WTMM analysis for the stack voltage signal acquired under nominal operating conditions is reported in Fig. 4. The singularities of the studied voltage signal provide $\tau(q)$ values with a curved q-dependency and the singularity spectrum is in the form of concave arc. So, we conclude that the studied voltage signal exhibits multifractal organization (set of self-similar structures as in the case of MBM(x), Fig. 2(b)) (right column)).

In Fig. 5, two average singularity spectra with standard deviation values computed on 10 voltage signals are displayed. The first one is obtained at nominal operating conditions (see Fig. 5 on the left side) and the second one in poor operating conditions with FSC = 1.3 (see Fig 5 on the right side). The curves indicate clear differences in the values of the multifractal parameters h_0, h_{min}, h_{max}, and width Δh. So, it can be noticed that the average values of h_0 (0.68 ± 0.08), h_{min} (0.17 ± 0.08), and h_{max} (1.33 ± 0.09) measured in poor conditions with FSC = 1.3, are lower than those obtained at nominal operating conditions (h_0 = 0.98 ± 0.10; h_{min} = 0.62 ± 0.11; h_{max} = 1.53 ± 0.17). These results reveal a high multifractality and irregularity degree of the voltage signal enhanced by the poor operating conditions resulting from cathode flow fault. Therefore, the multifractal parameters can be used as discriminant parameters.

The typical singularity spectra obtained from the investigated PEMFC operated in the four different conditions are displayed in Fig. 6. As we can see, the curves are well separated by their locations. Therefore, the four curves can be easily distinguished. After analyzing and comparing the multifractal parameters (listed in Table 3) obtained in the nominal operating conditions (Ref) to those estimated in the three situations of poor operating conditions, we can conclude that:

- the average singularity spectrum resulting for FSA = 1.3 (anode flow fault) exhibits regular regions close to those measured at nominal conditions (closed h_{max} values) and more irregular regions with less regularity expressed by a lower value of h_{min},
- the inlet gas pressure fault impacts the voltage signal by making it more regular: higher values of h_{min}, h_0, and h_{max} are obtained,
- the cathode flow fault impacts strongly the stack voltage morphology making it very irregular and more non-uniform. This comment can be done by interpreting the lower values of h_{min}, h_0, and h_{max} and a larger spectrum width.

To relate the results of the multifractal analysis to the physical phenomena of the FC, electrochemical impedance spectra were measured for the four operating conditions (Fig. 6). The estimated internal and polarization resistances (high and low frequency pure resistances) are listed in Table 4.

The polarization resistance growth in the situation of oxygen depletion (FSC = 1.3) is mainly a consequence of the difficulty of the oxygen to diffuse from the FC bipolar plates to the electrodes. This situation leads to water accumulation in the stack. The obtained EIS spectrum is enlarged. The singularity spectrum is shifted to the left to reveal the high irregularity of the voltage generated by the FC.

On the other hand, the EIS spectrum resulting in the situation of hydrogen depletion (FSA = 1.3) is almost superposed to those measured at nominal operating conditions (Ref). So, the EIS measures do not offer very clear discrimination between the two operating situations. However, this discrimination is more possible through the multifractal parameters h_{min}, h_0 and Δh.

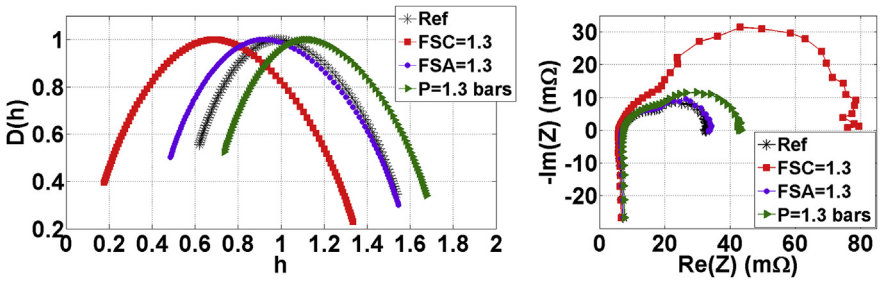

Fig. 6 – Typical curves of: singularity spectra (left side) and electrochemical impedance spectra, obtained at nominal operating conditions (Ref) and in poor operating conditions (fault modes) (right side).

Table 3 – Multifractal parameters (average ± std) obtained in the four operating conditions.

Operating conditions	h_0	h_{min}	h_{max}	Δh
Nominal conditions	0.98 ± 0.10	0.62 ± 0.11	1.53 ± 0.17	0.92 ± 0.23
FSC fault (FSC = 1.3)	0.68 ± 0.08	0.17 ± 0.08	1.33 ± 0.09	1.16 ± 0.15
FSA fault (FSA = 1.3)	0.91 ± 0.16	0.48 ± 0.11	1.54 ± 0.18	1.06 ± 0.15
Pressure fault (P = 1.3 bars)	1.11 ± 0.07	0.73 ± 0.07	1.68 ± 0.23	0.94 ± 0.25

Finally, the drop-down of the inlet gases pressure causes a slight increase of the polarization resistance (see Table 4). The measured singularity spectrum is clearly separated from the reference one (Ref). The stronger regularity observed on the voltage signal morphology in this situation is probably linked with effects of the control laws applied for the back pressure regulator.

The results obtained through the singularity spectra are very promising and encouraging to develop a more complete diagnosis strategy based on multifractal parameters in future works. To give an idea of a possible outlook reserved to the results presented in this paper, a summarized scheme is displayed in Fig. 7. The multifractal parameters can be classified using the K-Nearest Neighbor method (KNN) in order to identify the failures.

5. Conclusion

One approach to characterize a FC generator is the recording of temporal voltage signals which reflect the state of the system for different operating conditions. This work is dedicated to the measurement and analysis of stamped singularities on the voltage signal of a PEMFC stack operated under different constraints. The spatial and temporal variations of the studied signal indicate a multifractal structure of the PEMFC voltage. For the experimental parameter range explored, the analysis of the singularities spectra results highlights the following cause-effect relationships:

- A decrease of the cathode stoichiometry rate (FSC = 2 ê FSC = 1.3) induces a high irregularity of the FC voltage signal.
- A decrease of the anode stoichiometry rate (FSA = 1.5 ê FSA = 1.3) affects slightly the regularity of the stack voltage signal.
- A diminution of the inlet gas pressures (P = 1.5 bars abs.ê P = 1.3 bars abs) leads to a higher regularity of the voltage signal.

Table 4 – Internal and polarization stack resistances (average ± std) obtained in the four operating conditions.

Operating conditions	Internal resistance (m Ω)	Polarization resistance (m Ω)
Nominal conditions	6.65 ± 0.17	33.09 ± 0.53
FSC fault (FSC = 1.3)	5.99 ± 0.12	77.54 ± 1.42
FSA fault (FSA = 1.3)	6.90 ± 0.25	33.80 ± 1.65
Pressure fault (P = 1.3 bars)	7.18 ± 0.04	43.35 ± 0.42

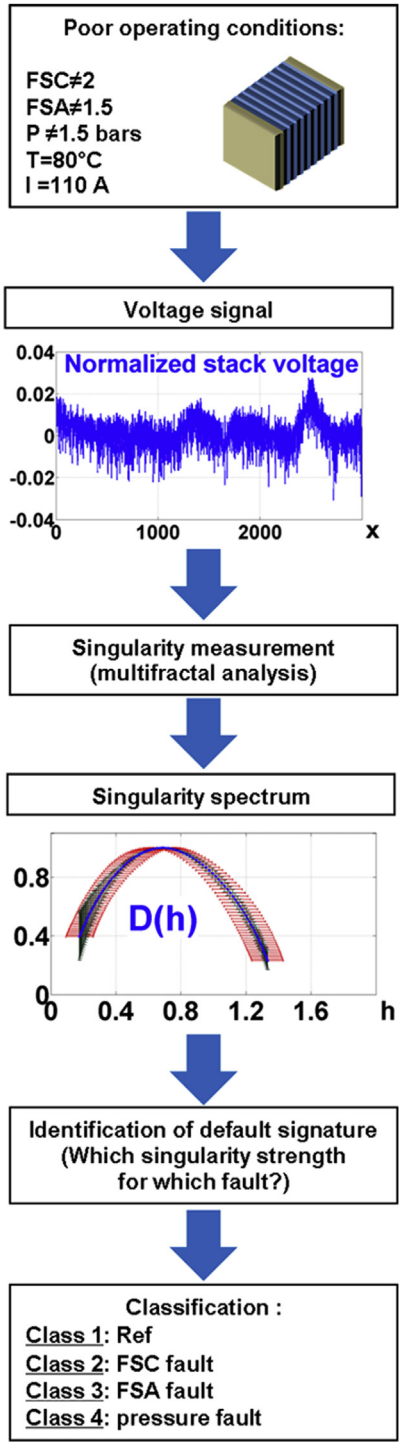

Fig. 7 – The different steps of the proposed FC diagnosis strategy based on voltage singularity analysis.

The obtained results demonstrate that the multifractal spectrum based on WTMM is effective to extract the incipient fault features during the PEMFC operating. The suggested method is a promising non-intrusive and low cost diagnostic tool (i.e. no EIS instrument is needed) to achieve on-line characterizations of dynamical FC behaviors. It offers an interesting computational performance for implementation in real time. In fact, the computing time is estimated at about 7 s for a voltage profile covering 3000 time points (about 5 min) under computer system characteristics of: Intel® Core™ i7-2960 XM, CPU @ 2.7 GHz, RAM:16 GO.

These results encourage us to further develop our diagnosis tool by considering other faults such as: monoxide Carbone poisoning at FC anode, temperature failure on the FC cooling circuit, and faults combination (by considering two or more failures simultaneously during the FC operation).

Acknowledgments

The French National Research Agency (ANR) is gratefully acknowledged for its support through the funding of the DIAPASON2 project.

Nomenclature

$B_x(s)$	volume element of size s and centered at x
c	constant
$D(h)$	singularity (or multifractal) spectrum
E_h	set of iso-Hölder points
FSC	cathode stoichiometry factor
FSA	anode stoichiometry factor
h	Hölder exponent
h_0	Hölder exponent for $q = 0$
h_{min}	Hölder exponent for $q = +3$
h_{max}	Hölder exponent for $q = -3$
$h(x)$	Hölder function
MBM(x)	multifractional Brownian Motion function
P	inlet gas pressures (bars)
q	order of statistical moments
$W_\psi(X)$	wavelet transform of the signal X
$\mathcal{W}_h(x)$	Weierstrass function
$Z(q, s)$	partition function
$\tau(q)$	scaling function
μ	measure
$\psi(x)$	wavelet function

REFERENCES

[1] Ang SMC, Fraga ES, Brandon NP, Samsatli NJ, Brett DJL. Fuel cell systems optimization- methods and strategies. Int J Hydrogen Energy 2011;36(22):14678–703.
[2] Chachuat B, Mitsos A, Barton PI. Optimal design and steady-state operation of micro power generation employing fuel cell. Chem Eng Sci 2005;60(16):4535–56.
[3] Xue D, Dong Z. Optimal fuel cell system design considering functional performance and production costs. J Power Sources 1998;76(1):69–80.
[4] Weber C, Maréchal F, Favrat D, Kraines S. Optimization of an SOFC-based decentralized polygeneration system for providing energy services in an office-building in Tokyo. Appl Therm Eng 2006;23(13):1409–19.
[5] Wang Yun, Chen Ken S, Mishler Jeffrey, Cho Sung Chan, Adroher Xavier Cordobes. A review of polymer electrolyte membrane fuel cells: technology, applications and needs on fundamental research. Appl Energy 2011;88(4):981–1007.
[6] Costamagna P, Srinivasan S. Quantum jumps in the PEMFC science and technology from the 1960s to the year 2000: part II. Engineering technology development and application aspects. J Power Sources 2001;102(1–2):253–69.
[7] Radev I, Koutzarov K, Lefterova E, Tsotridis G. Influence of failure modes on PEFC stack and single cell performance and durability. Int J Hydrogen Energy 2013;38(17):7133–9.
[8] Zhang S, Yuan X, Wang H, Walet M, Zhu H, Shen J, et al. A review of accelerated stress tests of MEA durability in PEM fuel cells. Int J Hydrogen Energy 2009;34(1):388–404.
[9] Yousfi-Steiner N, Moçotéguy Ph, Candusso D, Hissel D, Hernandez A, Aslanides A. A review on PEM voltage degradation associated with water management: Impacts, influent factors and characterization. J Power Sources 2008;183(1):260–74.
[10] Yousfi-Steiner N, Moçotéguy Ph, Candusso D, Hissel D. A review on polymer electrolyte membrane fuel cell catalyst degradation and starvation issues: causes, consequences and diagnostic for mitigation. J Power Sources 2009;194(1):130–45.
[11] Lim CY, Haas HR. A diagnostic method for an electrochemical fuel cell and fuel cell components. WO Patent March 2006. 2,006,029,254.
[12] Wruck WJ, Machado RM, Chapman TW. Current interruption-instrumentation and applications. J Electrochem Soc 1987;134(3):539–46.
[13] Ivers-Tiffe E, Weber A, Schichlein A. Electrochemical impedance spectroscopy. In: Vielstich W, Gasteiger HA, Lamm A, editors. Handbook of fuel cells: fundamentals, technology and applications, vol. 2. New York: Wiley; 2003. pp. 220–35.
[14] Ciureanu M, Roberge R. Electrochemical impedance study of PEM fuel cells. Experimental diagnostics and modeling of air cathodes. J Phys Chem B 2001;105(17):3531–9.
[15] Chen J, Zhou B. Diagnosis of PEM fuel cell stack dynamic behaviors. J Power Sources 2008;177(1):83–95.
[16] Yousfi Steiner N, Hissel D, Moçoteguy P, Candusso D. Non-intrusive diagnosis of polymer electrolyte fuel cells by wavelet packet transform. Int J Hydrogen Energy 2001;36(1):740–6.
[17] Kim Jonghoon, Lee Inhae, Tak Yongsug, Cho BH. State-of-health diagnosis based on hamming neural network using output voltage pattern recognition for a PEM fuel cell. Int J Hydrogen Energy 2012;37(5):4280–9.
[18] Riascos Luis Alberto M, Simoes Marcelo G, Miyagi Paulo E. A Bayesian network fault diagnostic system for proton exchange membrane fuel cells. J Power Sources 2007;165(1):267–78.
[19] Kimiagar S, Sadegh Movahed M, Khorram S, Sobhanian S, Reza Rahimi Tabar M. Fractal analysis of discharge current fluctuations. J Stat Mech 2009;03:P03020.
[20] Arneodo A, Bacry E, Graves PV, Muzy JF. Characterizing long-range correlations in DNA sequences from wavelet analysis. Phys Rev Lett 1995;74(16):3293–6.
[21] Ivanov PC, Rosenblum MG, Peng CK, Mietus J, Havlin S, Stanley HE, et al. Scaling behaviour of heartbeat intervals obtained by wavelet-based time-series analysis. Nature 1996;383(6598):323–7.
[22] Talu S. Multifractal geometry in analysis and processing of digital retinal photographs for early diagnosis of human diabetic macular edema. Curr Eye Res 2013;38(7):781–92.

[23] Benouioua-Ait Aouit D, Ouahabi A. Nonlinear fracture signal analysis using multifractal approach combined with wavelets. Fractals J (Complex Geometry Patterns Scaling Nat Soc) 2001;19(2). ISSN: 1793-6543:175–83.
[24] Lin J, Chen Q. Fault diagnosis of rolling bearing based on multifractal detrended fluctuation analysis and Mahalanobis. Mech Syst Signal Process 2013;38:515–33.
[25] Arneodo A, Decoster N, Roux SG. A wavelet-based method for multifractal image analysis. I. Methodology and test applications on isotropic and anisotropic random rough surfaces. Eur Phys J B – Condens Matter Complex Syst 1999;15(3):567–600.
[26] Tanner CW, Work KL. Fractal current distribution structures for thin electrolyte supported fuel cells. Electrochem Soc Trans (ECS) 2011;35(1):533–42.
[27] Istas J, Lang G. Quadratic variations and estimation of the local Hölder index of a Gaussian process. Annales de l'Institut Henri Poincaré (B) Probabilités et Statistiques 1997;33:407–36.
[28] Mallat SG, Hwang WL. Singularity detection and processing with wavelets. IEEE Trans Inf Theory 1992;38(2):617–43.
[29] Wendt H, Abry P, Jaffard S. Bootstrap for empirical multifractal analysis. IEEE Signal Process Mag 2007;24(4):38–48.
[30] Jaffard S. Wavelet techniques in multifractal analysis. In: Lapidus M, van Frankenhuysen M, editors. Fractal geometry and applications: a Jubilee of Benoit Mandelbrot. Proceedings of symposium in pure mathematics 2004.
[31] Hissel D, Péra MC, Candusso D, Harel F, Bégot S. Characterization of polymer electrolyte fuel cell for embedded generators. Test bench design and methodology. In: Zhang Xiang-Whu, editor. Chapter of advances in fuel cells, Research Signpost. North Carolina State Univ; 2005. pp. 127–48.
[32] Frish U, Parisi G. Fully developed turbulence and intermittency in geophysical fluid dynamics and climate dynamics. Amsterdam: North-Holland; 1985.
[33] Diego JM, Martinez-Gonzales E, Sanz JL, Mollerach S, Mart VJ. Partition function based analysis of cosmic microwave background maps. Mon Not R Astron Soc 1999;306(2):427–36.
[34] Kantelhardt JW. Fractal and multifractal time series. In: Mathematics of complexity and dynamical systems. New York: Springer; 2011. pp. 463–87.